



Chapter V

Discussion

5.1 The liquid phase formation temperatures

From the temperature-time and the resistivity-time data of each batch, the resistivity versus temperature curves were plotted as shown in figure 5.1 (for the examples of batch 05). This newly plotted curves are used to determine the onset temperature (T_{On}) and the end temperature (T_{end}) of primary liquid phase formations at different positions in the batch blanket.

R-T PLOT OF BATCH 05

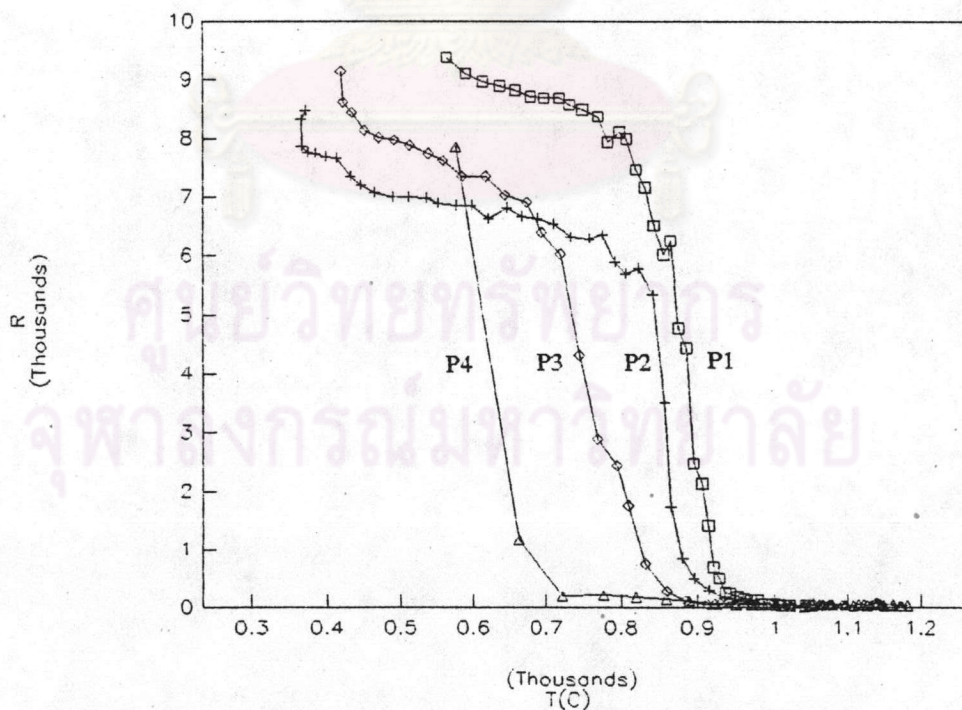


Fig. 5.1 Resistivity vs. temperature curve at different positions P_1 to P_4 in batch 05.

From each curve, T_{on} and T_{end} can be determined by creating two tangent lines (see figure 5.2), the intersection of these lines indicates T_{on} and the end of the sharply dropping tangent line indicates T_{end} . The data of T_{on} and T_{end} of all batches are summarized in table 5.1. Time demand to reach the end temperature of primary liquid phase (t_{end}) was also determined.

R-T PLOT OF BATCH 07

POSITION P1

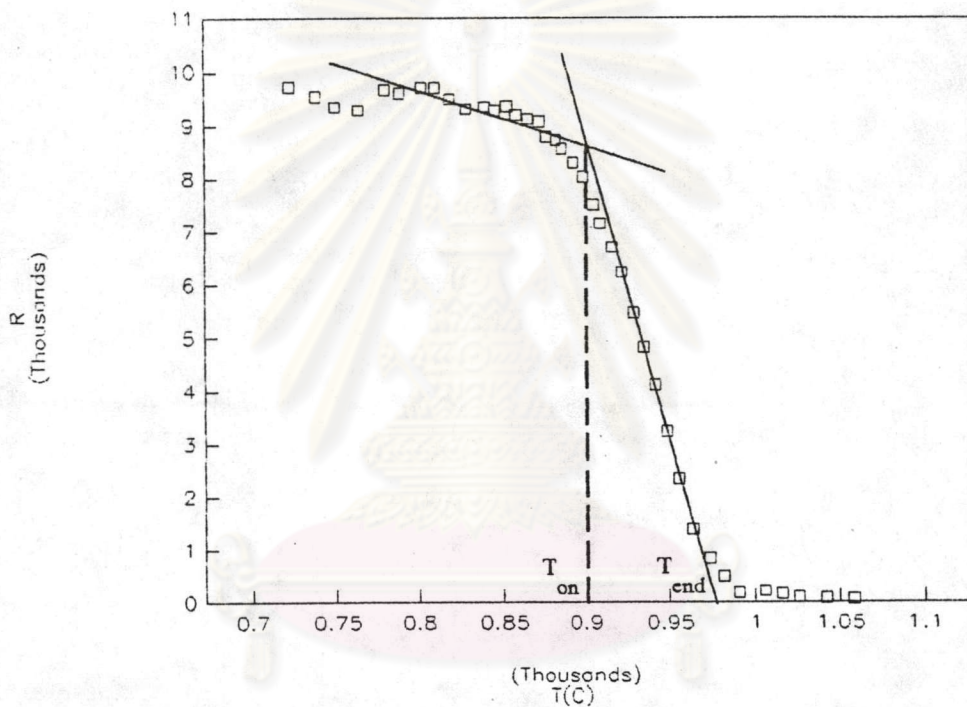


Fig. 5.2 Resistivity vs. temperature curve at position P_1 in batch 07; resistivity (R) is given in mV voltage drop and T is given in $^{\circ}\text{C}$.

Tab. 5.1 Summarized data of the onset temperature (T_{on}), the end temperature (T_{end}), and the time demand for major primary liquid phase formation (t_{end}) at positions P_1 to P_4 of all batches.

Batch no.	<-- T_{on} in $^{\circ}C$ -->				<-- T_{end} in $^{\circ}C$ -->				<- t_{end} in min ->			
	P_1	P_2	P_3	P_4	P_1	P_2	P_3	P_4	P_1	P_2	P_3	P_4
01	870	1017	820	1000	900	1025	870	1110	-	-	3	7
02	805	750	840	1002	935	815	870	1050	-	16	-	-
03	850	800	770	975	865	890	900	1030	-	21	8	3
04	840	880	770	730	950	880	810	830	25	2	15	2
05	840	840	710	580	930	875	805	675	25	30	20	1
06	880	900	800	630	935	980	915	720	25	33	20	3
07	900	850	750	700	975	945	840	765	32	35	22	4
08	825	820	770	715	965	910	835	815	30	27	13	2
09	820	380	740	750	885	385	805	830	41	19	3	4
10	920	800	760	635	955	875	845	715	26	30	20	3
11	860	750	680	640	930	820	770	715	26	24	16	3
12	840	800	650	875	920	865	750	920	26	25	7	2

To clearly explain the meaning of the onset and end temperature of primary liquid phase formation, figure 5.3 a to c is used. This can be divided into 3 steps. At first, there is no liquid, resistivity value remains very high due to solid state mobility and grain-to-grain contact (a). Secondly, primary liquid phase begins to form, resistivity will gradually decrease due to increased alkali ion mobility, however, grain-to-grain contact still controls the result (b). This step indicated as onset temperature. Finally, an intercon-

nected liquid phase occurs (c), resistivity is immediately dropping and the end temperature is reached.

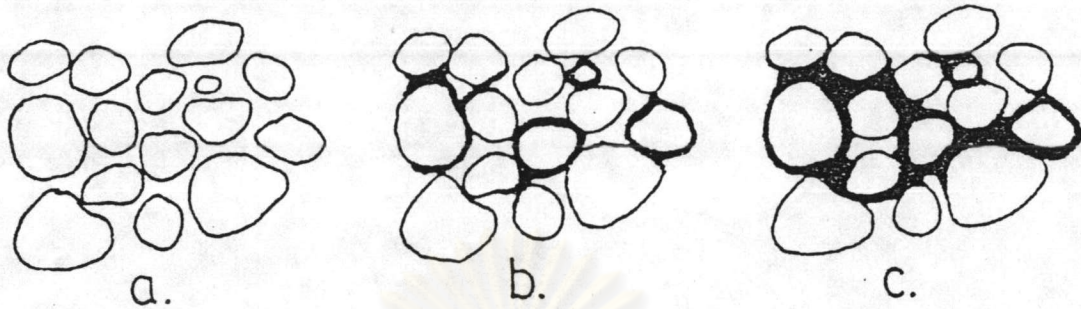


Fig. 5.3 Illustration of absence, (a), onset, (b), and end (c) temperature of primary liquid phase formation.

From the onset and the end temperature data listed in table 5.1, the onset and end temperature for temperature range below 950 °C. They are plotted as a function of positions in the batch blanket as shown in figure 5.4; average value was also plotted.

Tend and Ton vs. Position

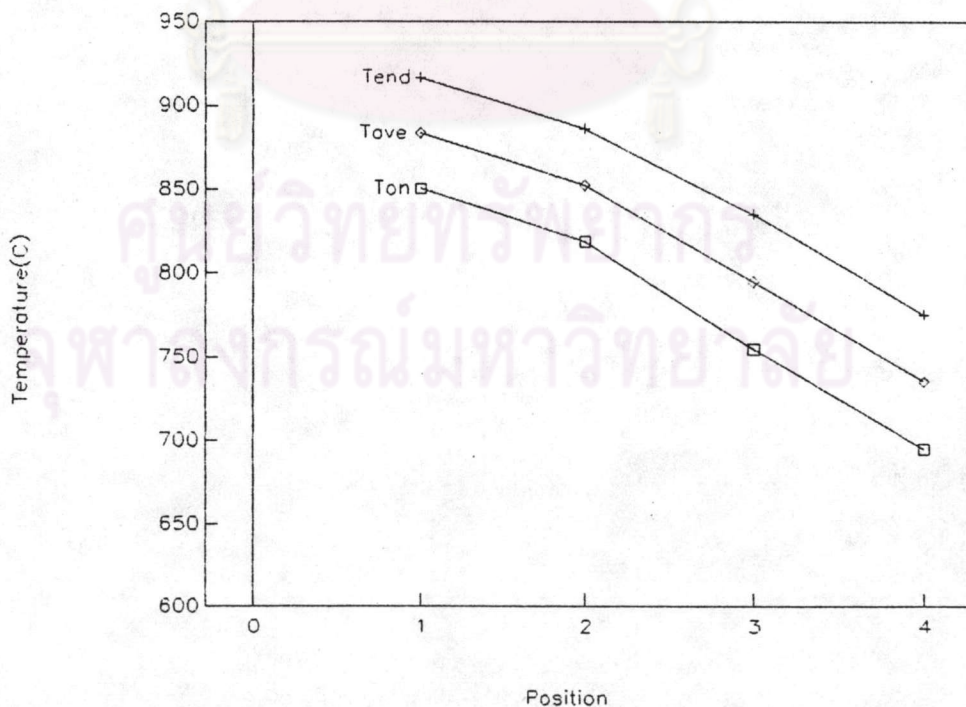


Fig. 5.4 Variation of primary liquid phase formation temperature at different positions in the batch blanket.

The primary liquid phase is likely to occur in the temperature range 850 to 917 °C for the position P₁, 819 to 886 °C for P₂, 755 to 835 °C for P₃, and 850 to 917 for P₄. This means primary liquid phase formation temperature is different according to the position in the batch blanket. This finding already seen from figure 5.1 does not go along with the many models that assumed a uniform reaction temperature all over the batch blanket. The primary liquid phase formation temperature of position P₄ has the lowest value. This position was placed nearest to the surface of the batch blanket and received the highest heat flux. For all batches, the temperature difference between onset and end temperature was derived. This meets an approximate value of 80 °C and can be written as a simple equation;

$$T_{\text{end}} - T_{\text{on}} \sim 80 \text{ } ^\circ\text{C}$$

This equation implies that T_{end} and T_{on} belong to the same process. The equation is very useful to estimate the value of T_{end} or T_{on} when only one value is known.

5.2 The variation of heating rate at different positions

From the data acquired in the appendix D, the heating rate of all batches at different positions from P₁ to P₄ was calculated and listed in the appendix E. Figure 5.5 shows the relation between local heating rate of all batches and a position in the batch blanket.

Heating rate vs. Position

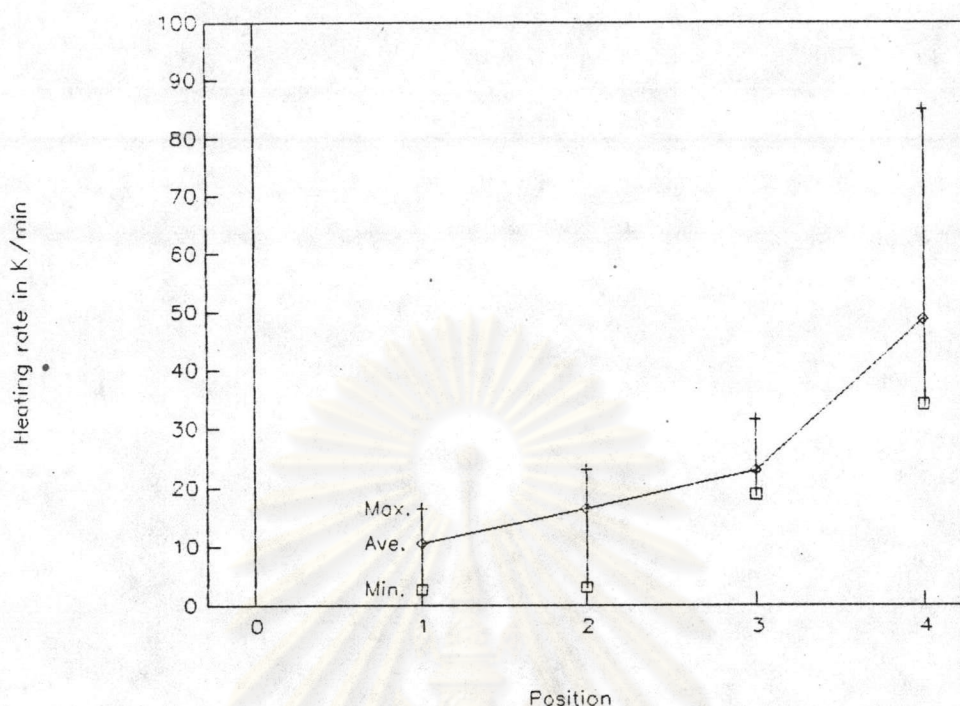


Fig. 5.5 The Variation of heating rate (given in K/min) according to different positions in the batch blanket.

For the example of batch (05), the heating rates at positions P_1 , P_2 , P_3 , and P_4 are equal to 13.6 K/min, 18.9 K/min, 23.6 K/min, and 44.9 K/min respectively. Position P_4 which has the highest heating rate, followed P_3 , and P_2 , P_1 which have the lowest rate. This correlates to results from the previous section, for instance, the position P_4 has the highest heating rate and also has the lowest primary liquid phase formation temperature. This is still true yet for another positions. The question arise: How can the heating rate influence the temperature of melting. This is virtually impossible in system like ice/water. Yet, an earlier paper hit a very similar finding. A heat microscopic study by Riedel (1962) demonstrated how the heating rate influences the course of reaction between an individual soda ash particle which is in contact with both a quartz and a limestone particle. three diff-

erent cases by Riedel, together with some conclusions from this thesis are compiled.

Case 1. Fast heating.

Upon fast heating, the soda ash particle separates from the quartz and is absorbed by the limestone grain. So the primary melt is governed by the sub-system $\text{Na}_2\text{CO}_3\text{-CaCO}_3$ (eutectic at 785°C , reaction point at 817°C) leading to a quick formation of ternary $\text{Na}_2\text{O-CaO-SiO}_2$ melts (metastable eutectic at 765°C).

Case 2. Slow heating.

Upon slow heating, the soda ash grain separates from the limestone particle and exclusively reacts with the quartz. So the primary melt is governed by the sub-system $\text{Na}_2\text{CO}_3\text{-SiO}_2$ with primary melt occurring below between the eutectic at 837°C and 1088°C . So we can conclude that the formation of ternary $\text{Na}_2\text{O-CaO-SiO}_2$ does not take place as fast as via the soda lime route.

Case 3. High excess of soda ash.

The trends reported above become diluted when the amount of soda ash is high. The microscopic observations show that in this case, there is only one indistinguishable reaction among all three partners. Conclusions on the primary melt temperature are not clear yet. Figures 5.6 (a) and 5.6 (b) show the relation between the heating rate of all batches and the temperature of primary liquid phase formation, T_{on} and T_{end} . This finding is in agreement with the earlier results from microscopical experiments.

Ton vs. Heating rate

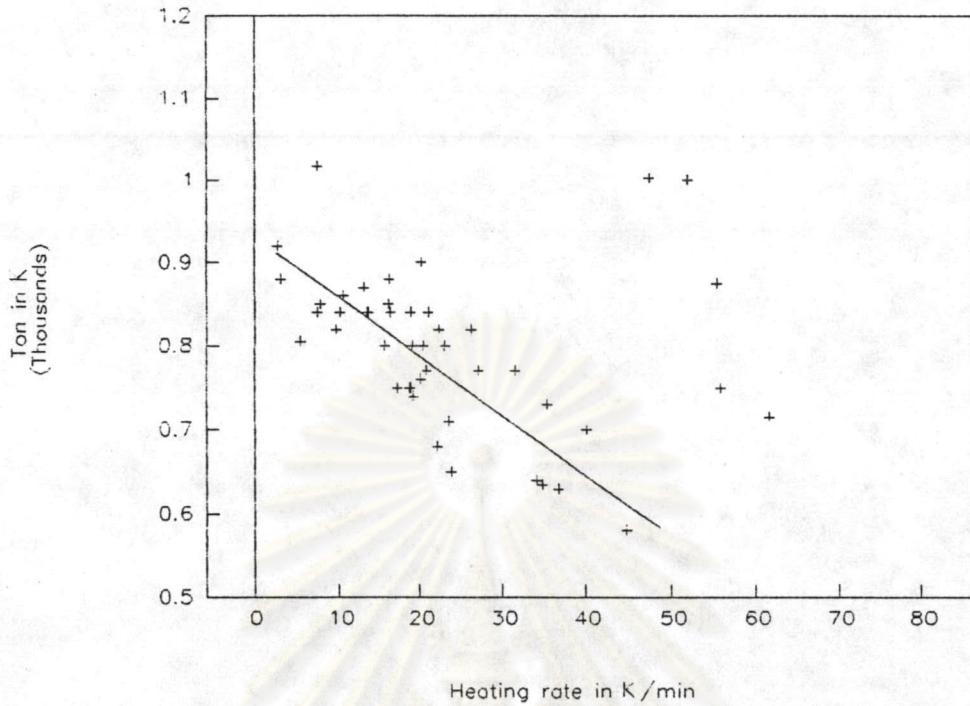


Fig. 5.6 (a) Relation between heating rate of all batches and onset temperature of primary liquid phase formation.

Tend vs. Heating rate

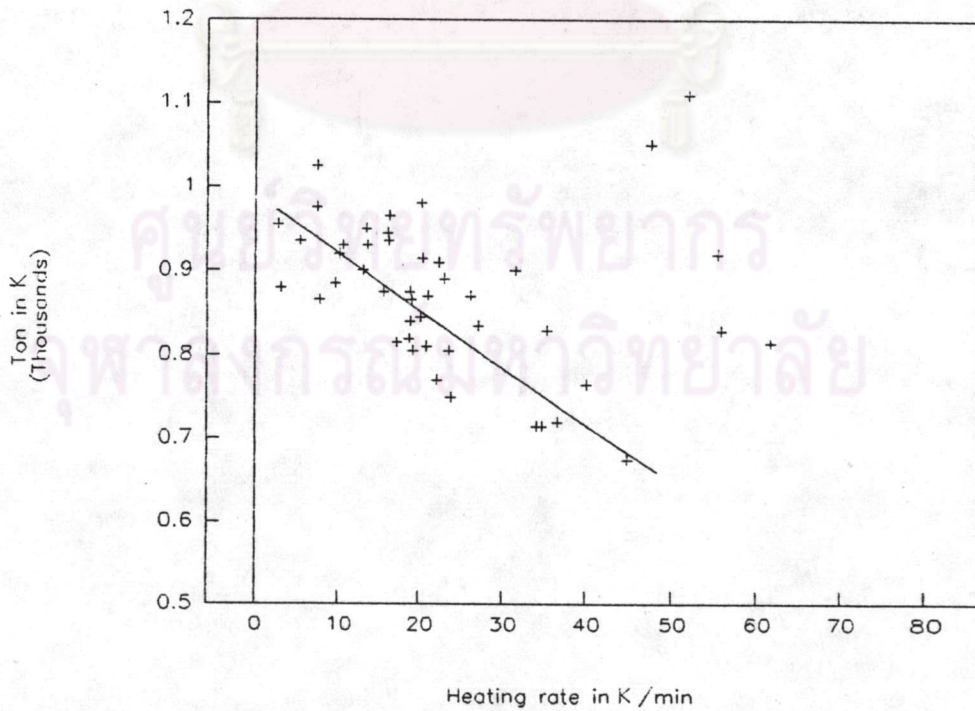


Fig. 5.6 (b) Relation between heating rate of all batches and end temperature of primary liquid phase formation.

Different approaches can be used to explain this phenomenon as shown in figure 5.7, plotted between heating rate and t_{end} . As expected when the heating rate increased, the time used for occurrence of primary liquid phase is decreased. However, if the heating rate was higher than a critical value, time demand would not decrease any more. In this case, the heating rate was no longer rate controlling.

Melting time vs. Heating rate

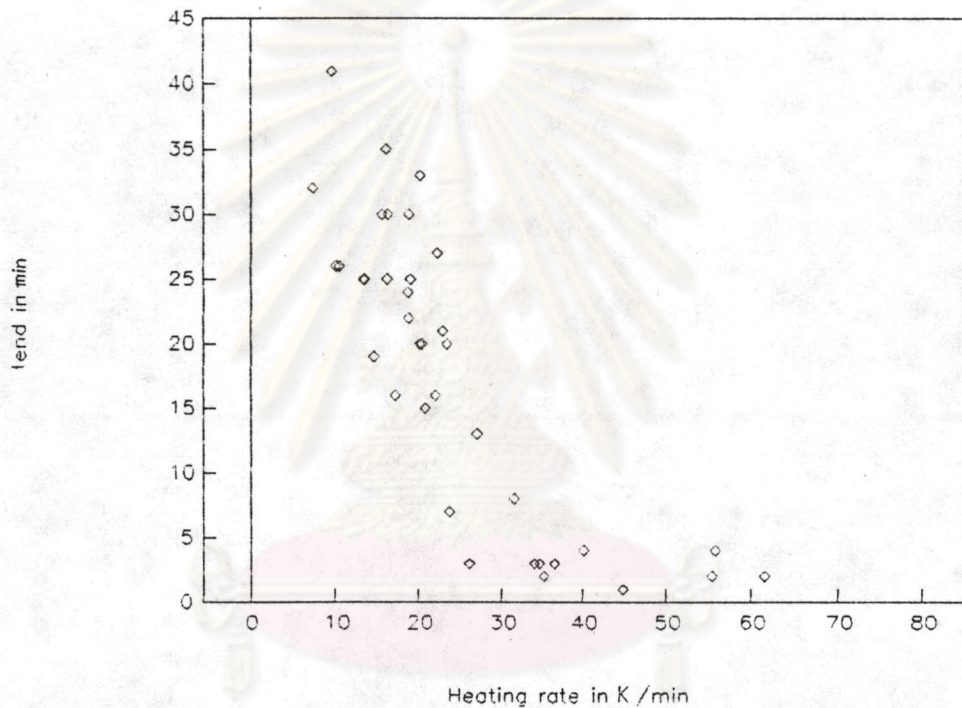


Fig. 5.7 Heating rate of all batches as a function of time demand for primary liquid phase formation (T_{end}).

5.3 Differential resistivity analysis

The resistivity-temperature curve of all batches (as shown in the appendix D), which display ups and downs, may be interpreted as signal fluctuations (i.e., noise). With little effort, the method could be upgraded to something like a "differential resistivity analysis" (DTR). However, an interpretation in terms of real effects related to real events occurring in the batch blanket will not be discussed in this

thesis. The main purpose of this section is to suggest a method useful to follow a reaction taking place in a blanket at realistic dimension. Until today, an investigation on thermal behavior of batch blanket is still limited to the well-known differential thermal analysis (DTA) method, which cannot handle samples over 5 g. This is very important if related to the industrial scale, because, the reactions taking place in a large scale are controlled by boundary conditions significantly different from the microscopic scale. Figure 5.8 compares resistivity-temperature plots for position P_1 of selected batches.

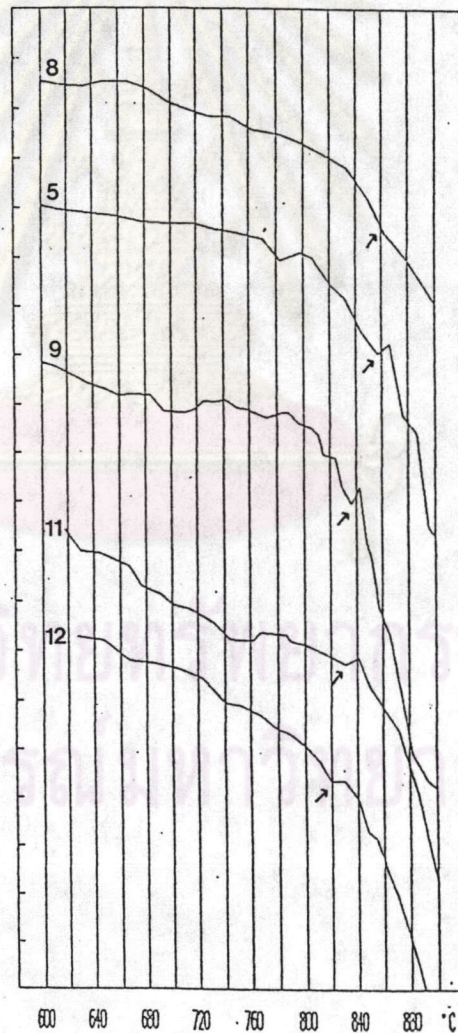


Fig. 5.8 Resistivity signals recorded from different batches in arbitrary units as a function of temperature; arrows marked is an example of a differential effect.

5.4 Isotherms and melting front in the batch blanket

From the temperature-time curve of all batches in the appendix F, the isotherms between 700 to 1000 °C in steps of 100 °C were determined as a function of time. The end temperature and time required for the formation of primary liquid phase were also plotted as melting front in the same diagram (all isothermal curves of individual batches are given in the appendix I). An interesting feature for most batches is that the lower part of the batch blanket is "dry" (liquid phase does not occur) for a long period of time (see figure 5.9). This means, new melt will be drained away immediately from the blanket and does not influencing the neighbouring upper layers of the batch blanket at all.

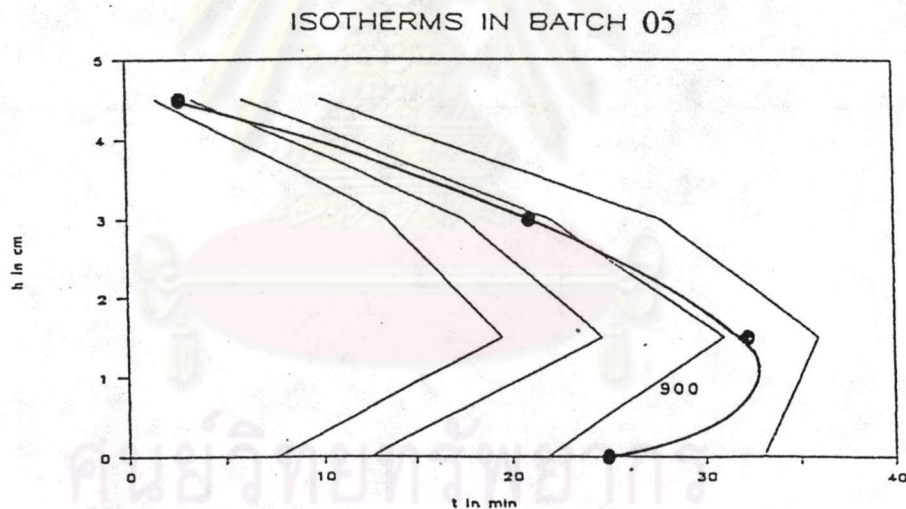


Fig. 5.9 Isotherm at 700 to 1000 °C and melting front of position P₁ P₄ in batch 05 plotted as a function of time.

In the oxidizing batches (batch 05 to 08) the melting front always cross the isotherm of 900 °C (also shown in figure 5.9). By contrast, in the reducing batches (batch 09 to 12), the melting front hardly cross the isotherm of 900 °C (see figure 5.10). This means that, reducing batches melt more easily. This may be due to the formation of

Na_2S by the sulphate and carbon reactions.

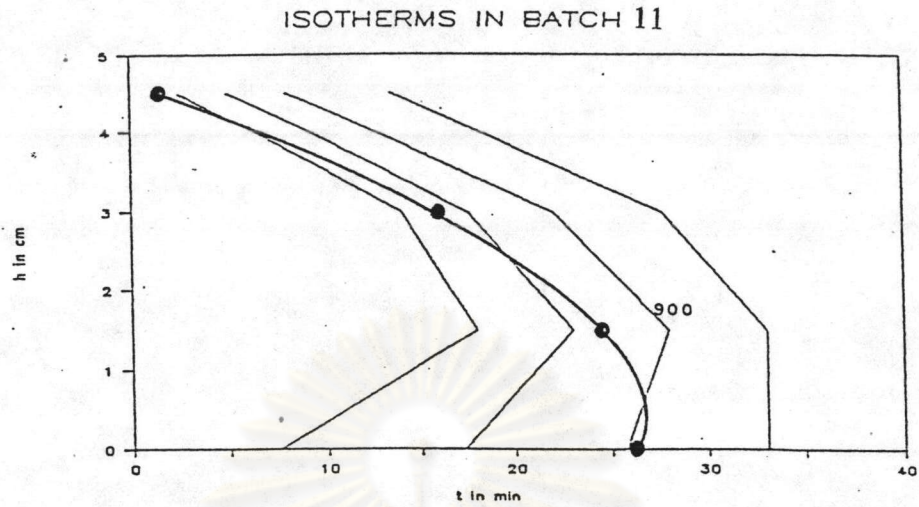


Fig. 5.10 Isotherm at 700 to 1000 °C and melting front of position P_1 - P_4 in batch 11 plotted as a function of time.

Figure 5.11 shows isotherms and a melting front of batch 01. This batch contains a high amount of soda ash and primary liquid phase was formed very quickly, however, the progress of the reactions was low due to the physical melting processes preferred over the chemical one. So we can conclude that, high amounts of soda ash are not beneficial for batch melting. In fact, a later inspection of the cross section of the rigid batch showed that a large number of quartz had been carried to the upper zone of the batch. This might also prove as an explanation for the inversed melting front: All soda drains to the bottom ($T_{\text{liq}} = 851 \text{ }^\circ\text{C}$) while in the upper part, soda depletion leads to increased T_{liq} .

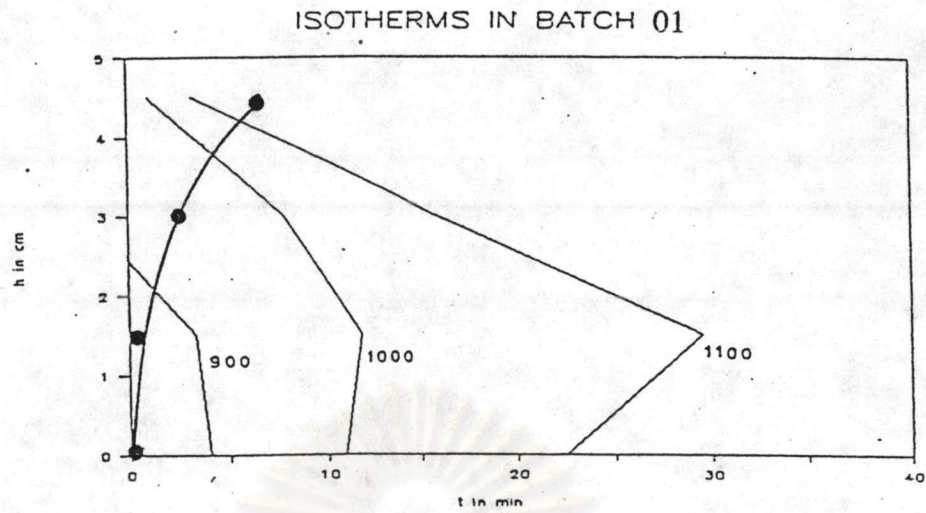


Fig. 5.11 Isotherm at 700 to 1000 °C and melting front of position P_1 - P_4 in batch 01 plotted as a function of time.



ศูนย์วิทยทรัพยากร
จุฬาลงกรณ์มหาวิทยาลัย